PROCEEDINGS B

royalsocietypublishing.org/journal/rspb

Research

Cite this article: Coussement L *et al*. 2023 Liver transcriptomic and methylomic analyses identify transcriptional mitogen-activated protein kinase regulation in facultative hibernation of Syrian hamster. *Proc. R. Soc. B* **290**: 20230368.
https://doi.org/10.1098/rspb.2023.0368

Received: 14 February 2023
Accepted: 2 May 2023

Subject Category:
Development and physiology

Subject Areas:
molecular biology, genomics, physiology

Keywords:
facultative hibernator, torpor, gene regulation, cell cycle, transcription factor-binding sites, DNA methylation

Author for correspondence:
Robert H. Henning
e-mail: r.h.henning@umcg.nl

†These authors contributed equally to this study.

Electronic supplementary material is available online at https://doi.org/10.6084/m9.figshare.c.6644096.

THE ROYAL SOCIETY PUBLISHING

Liver transcriptomic and methylomic analyses identify transcriptional mitogen-activated protein kinase regulation in facultative hibernation of Syrian hamster

Louis Coussement[1,†], Marloes M. Oosterhof[2,3,†], Victor Guryev[4], Vera A. Reitsema[2], Jojanneke J. Bruintjes[2], Maaike Goris[2], Hjalmar R. Bouma[2,5], Tim de Meyer[1], Marianne G. Rots[3] and Robert H. Henning[2]

[1]Department of Data Analysis and Mathematical Modelling, Faculty of Bioscience Engineering, Ghent University, B-9000 Ghent, Belgium
[2]Department of Clinical Pharmacy and Pharmacology, [3]Department of Pathology and Medical Biology, [4]European Research Institute for the Biology of Ageing, and [5]Department of Internal Medicine, University of Groningen, University Medical Center Groningen, 9713 GZ Groningen, The Netherlands

LC, 0000-0003-1736-4962

Hibernation consists of alternating torpor–arousal phases, during which animals cope with repetitive hypothermia and ischaemia-reperfusion. Due to limited transcriptomic and methylomic information for facultative hibernators, we here conducted RNA and whole-genome bisulfide sequencing in liver of hibernating Syrian hamster (*Mesocricetus auratus*). Gene ontology analysis was performed on 844 differentially expressed genes and confirmed the shift in metabolic fuel utilization, inhibition of RNA transcription and cell cycle regulation as found in seasonal hibernators. Additionally, we showed a so far unreported suppression of mitogen-activated protein kinase (MAPK) and protein phosphatase 1 pathways during torpor. Notably, hibernating hamsters showed upregulation of MAPK inhibitors (dual-specificity phosphatases and sproutys) and reduced levels of MAPK-induced transcription factors (TFs). Promoter methylation was found to modulate the expression of genes targeted by these TFs. In conclusion, we document gene regulation between hibernation phases, which may aid the identification of pathways and targets to prevent organ damage in transplantation or ischaemia-reperfusion.

1. Background

Hibernation is an adaptive strategy to cope with inadequate energy supply because of low food availability or challenging thermoregulatory conditions, and is characterized by metabolic suppression, lowering of body temperature (T_b) and cessation of locomotive activity during periods of torpor. Torpor periods are alternated with briefer arousal periods, an energetically expensive process restoring metabolism and T_b. Whereas hibernators tolerate the repetitive, drastic alterations in physiology during torpor–arousal cycles, similar alterations result in organ dysfunction and damage in non-hibernators such as rats and humans [1,2].

Numerous studies of hibernating mammals have revealed changes in gene expression. Transcriptome analysis across hibernation phases mainly in seasonal (i.e. non-hoarding) squirrels identified a switch in expression of metabolic genes to accommodate fatty acid oxidation throughout hibernation [3–6]. In contrast with seasonal hibernators, Syrian hamster (*Mesocricetus auratus*) is a facultative hibernator, which enters hibernation in response to environmental cues, such as lowering of ambient temperature and shortening of daylight, rather than being

Table 1. Total number of DEGs with FDR < 0.01 between the three investigated phases of hibernation. Direction of regulation is represented against the first group in the comparison. There is a significant difference in the number of up- and downregulated genes between phases ($p < 0.0001$, χ^2 test).

	SE versus TL		TL versus AE		SE versus AE		SE versus TL + AE	
total DEGs	272		137		435		508	
upregulated	124	45%	128	93%	270	60%	241	47%
downregulated	148	55%	9	7%	165	40%	267	53%

driven by an endogenous circannual rhythm [7]. Importantly, their facultative nature of hibernation might involve divergent pathways that may be exploited to prevent organ damage in the human setting. As no comprehensive transcriptomic studies in facultative hibernating species have yet been reported, we examined expression changes, as well as DNA methylation differences, in hibernating Syrian hamster. To investigate the metabolic aspect of facultative hibernation, we studied the liver of the Syrian hamster. Liver is considered a crucial organ in hibernation, as it accommodates the bulk of the metabolic changes from summer to hibernation [8]. Additionally, liver is the site of synthesis of enzymes involved in gluconeogenesis and ketone body formation, processes required for fuel generation during the hibernation season [9]. Therefore, we performed unbiased RNA sequencing and DNA methylation analysis in liver from summer, torpid and arousing Syrian hamster to explore mechanisms of hibernation initiation and organ protection in a facultative hibernator. To obtain the optimal contrasts between the expression of genes relevant to the transition from torpor to arousal and to limit effects of food intake on gene expression in this hoarding species, liver from aroused hamsters was obtained at early arousal (i.e. after 90 min of full rewarming). In addition to regulation of genes involved in metabolism switching, RNA transcription and cell proliferation, our results identified the suppression of the mitogen-activated protein kinase (MAPK) pathway in torpor and increased promoter methylation in binding sites/sequences of MAPK transcription factors (TFs) in arousal. These results provide additional evidence for the relevance of these TFs, as the limited enrichment of their targets may be explained by the inhibitive effect of DNA methylation on expression of non-responding TF target genes.

2. Results

(a) Analysis of gene expression differences between hibernation stages

Liver gene expression changes during the torpor–arousal cycle were analysed by comparing RNA-sequencing (RNA-seq) data of summer euthermic (SE) animals and the two hibernation stages, torpor late (TL) and arousal early (AE). The number of differentially expressed genes (DEGs) was 272 for SE versus TL, 137 for TL versus AE and 435 for SE versus AE (table 1). Number and overlap of genes during hibernation stages are summarized in a Venn diagram (figure 1*a*). The unique DEGs of SE versus TL, TL versus AE and SE versus AE were visualized by Volcano plots (figure 1*b–d*; full DEG lists available in electronic supplementary material, table S1). Of the DEGs, 394 were unique for a single comparison between stages; 225 were differentially expressed for two comparisons (figure 1*a*).

Next, the distribution of up- and downregulated DEGs was examined. In SE versus TL and SE versus AE, the number of up- and downregulated genes was almost equal, with a small excess of downregulated genes when comparing SE to TL (55%) and of upregulated genes when comparing SE to AE (60%; table 1). In striking contrast, the transition from TL to AE was characterized almost exclusively by upregulation of gene expression in AE, representing 93% of the 137 DEGs ($p < 2.2 \times 10^{-16}$, binomial test). Of the 128 upregulated DEGs between TL and AE, 63 were also upregulated in AE compared to SE, thus representing genes that are overexpressed specifically upon arousal.

Comparing SE to TL, two upregulated genes in TL had a remarkably low false discovery rate (FDR) and high fold change: pro-platelet basic protein and tubulin beta-1 chain (*PPBP*: 20-fold, *TUBB1*: 12-fold). In humans, mice [10] and 13-lined ground squirrel [11] (and therefore most likely also in hamsters), these two genes are mainly expressed in platelets, and their upregulation is in line with the storage of platelets in liver during torpor [12]. Also 5-aminolevulinate synthase (*ALAS2*) is a prominently upregulated gene in torpor compared to SE and AE (5-aminolevulinate synthase: fivefold). *ALAS2* encodes an enzyme which catalyses the first step in the haeme biosynthetic pathway, although translation is dependent on adequate iron supply [13]. Three genes in the top 10 of most significantly downregulated genes in TL versus SE (ranking 9th, 11th and 15th in electronic supplementary material, table S1) encode regulatory subunits of protein phosphatase 1 (PP1) (*PPP1R3C* and *PPP1R10* (both sixfold downregulated) and *PPP1R3B* (fivefold downregulated)). These subunits remained downregulated in AE compared to SE. In liver, PP1 accelerates glycogen synthesis and coordinates carbohydrate storage [14]. Downregulation of these subunits in torpor may thus contribute to the shift from glucose to fatty acid metabolism as part of the metabolic rewiring in hibernation.

DEGs downregulated in both TL and AE compared to SE, largely represent innate immune response genes and three benzaldehyde dehydrogenase [NAD(P)+] activity genes. The immune response was suppressed during torpor through a strong reduction in circulating leucocyte numbers [15], decreased phagocytic capacity and complement activity [16], with rapid restoration of these processes during arousal. Thus, our data support the notion that the immune system in liver of Syrian hamster remains suppressed during early arousal and is reactivated only late in arousal or even after hibernation [17]. This view is consistent with increased expression of tumour necrosis factor, alpha-induced protein 3 (*TNFAIP3*) in AE, a strong inhibitor of the Toll-like receptor

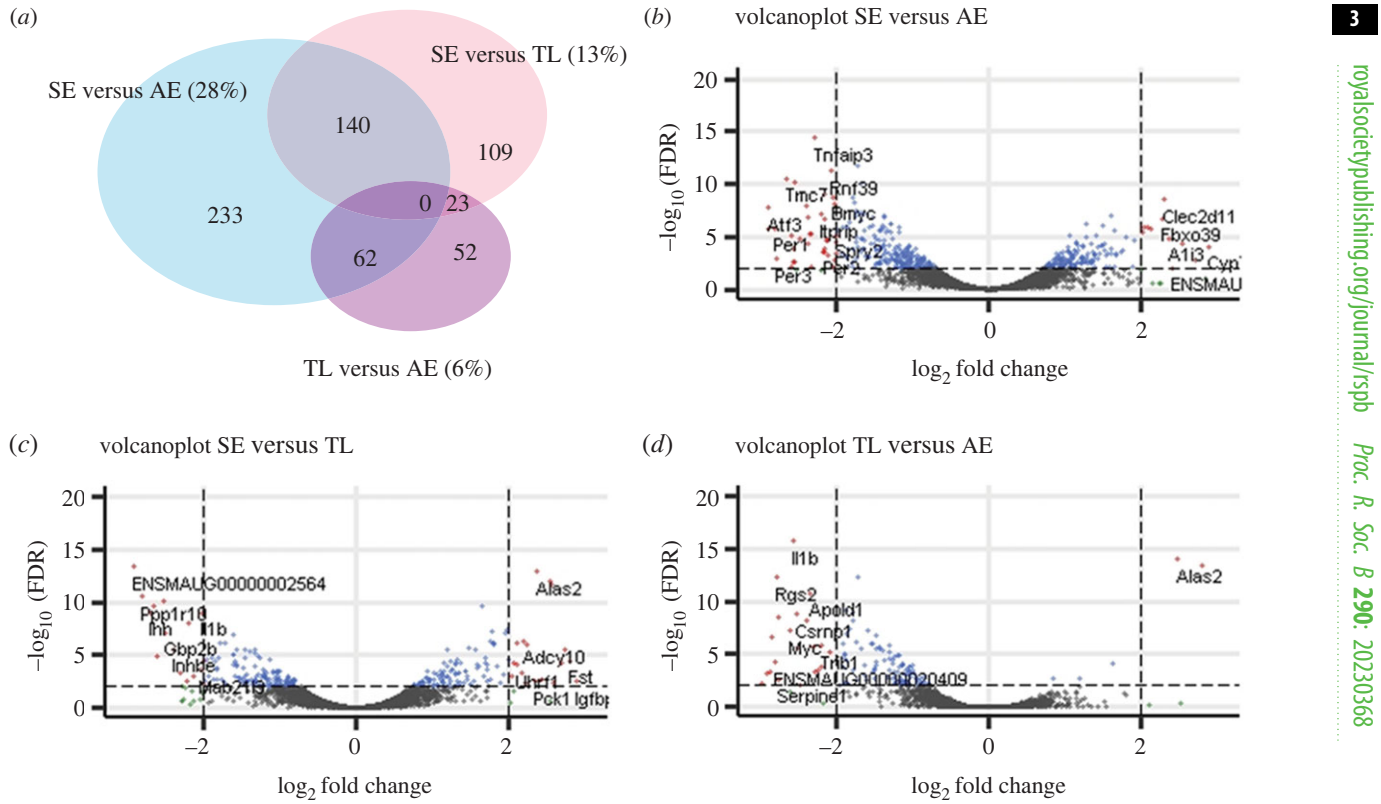

Figure 1. DEGs in the RNA-sequencing data. (*a*) Venn diagram of DEGs (FDR < 0.01) identified SE versus TL, TL versus AE and SE versus AE. (*b–d*) Volcano plots of genes identified using RNA-seq for SE versus TL, TL versus AE and SE versus AE, respectively. The FDR cut-off line was FDR < 0.01 (vertical dashed line). Vertical dashed lines represent cut-off of logFC of −2 and +2.

pathway and protective against cell death in renal cold ischaemia-reperfusion injury [18].

(b) Gene ontology of differentially expressed genes

To identify cellular pathways associated with DEGs between specific hibernation stages, gene ontology (GO) and Kyoto encyclopaedia of genes and genomes (KEGG) pathways analyses were performed (electronic supplementary material, table S2). First, to identify processes possibly regulating initiation and maintenance of hibernation, up- and downregulated genes in SE versus both TL and AE were examined. Expectedly, gene set enrichment analysis includes metabolic GO terms (e.g. lipid response), several metabolic processes and hormonal response (figure 2*d*; electronic supplementary material, table S2). Many hibernating species shift from glucose to fatty acid metabolism when entering torpor [5]. GO analysis validated this metabolic shift towards lipid metabolism in TL compared to SE, as GO terms including 'response to lipid' and 'cellular response to hormone/insulin stimulus' were covered by the DEGs in SE versus TL (figure 2*a*). In addition, KEGG pathway analyses suggested insulin resistance as a well-represented process in SE versus TL animals (electronic supplementary material, table S2). In homeostatic environments, insulin helps control blood glucose levels, promoting blood glucose uptake and storage as glycogen. During hibernation, however, animals become relatively resistant to insulin, shifting the metabolic processes from glycolysis to glycogenolysis and gluconeogenesis as important sources for glucose in torpor. This is indeed reflected by the upregulation of a variety of genes in torpor (the phrasing 'up- or downregulation in torpor' refers to all genes in those contrasts that include torpor; this interpretation is used throughout the manuscript). Upregulated genes included α-glucosidase (*GAA*), glycogen phosphorylase (*PYG*), peroxisome proliferator-activated receptor gamma coactivator 1-alpha, phosphoenolpyruvate carboxykinase 1 and glucose 6-phosphate (electronic supplementary material, table S1). In addition, glycolysis is inhibited during torpor and early arousal by the downregulation of the gene encoding the rate-limiting enzyme, germinal centre kinase 1 (*GCK1*). Upregulation of pyruvate dehydrogenase kinase 4 in TL and AE versus SE (electronic supplementary material, table S1) inhibits pyruvate dehydrogenase and limits conversion of pyruvate into acetyl-CoA, thus repressing glucose-derived oxidative phosphorylation in mitochondria and supporting fat metabolism, as shown previously in fasted and starved mammals [19].

Although metabolic genes clearly undergo substantial regulation during hibernation, the most prominent regulation in all contrasts between stages was observed in the MAPK pathway, particularly its MAPK 1/3 (extracellular signal-regulated kinase (ERK1/2)) cascade (figure 3). Upregulated DEGs in both TL and AE versus SE, comprised upregulation of inhibitors of the MAPK pathway (multiple dual-specificity phosphatase (DUSP) *DUSP1*, *DUSP3*, *DUSP4*, *DUSP8*, *DUSP10* and *SPRY2*; electronic supplementary material, table S1). Further, the MAPK pathway is also represented genes downregulated in TL compared to AE (e.g. sprouty related EVH1 domain containing 2, ephrin type-A receptor 4), suggesting differential regulation of specific downstream cascades during hibernation, including the p38 MAPK (p38MAPK), ERK1/2 and c-Jun-terminal kinase [20]. Collectively, overlap with DEG results implies a substantial inhibition of the MAPK pathway in TL versus SE (figure 4). Consistently, KEGG analysis confirmed the regulation of the MAPK pathway when comparing SE versus AE animals (electronic supplementary material, table

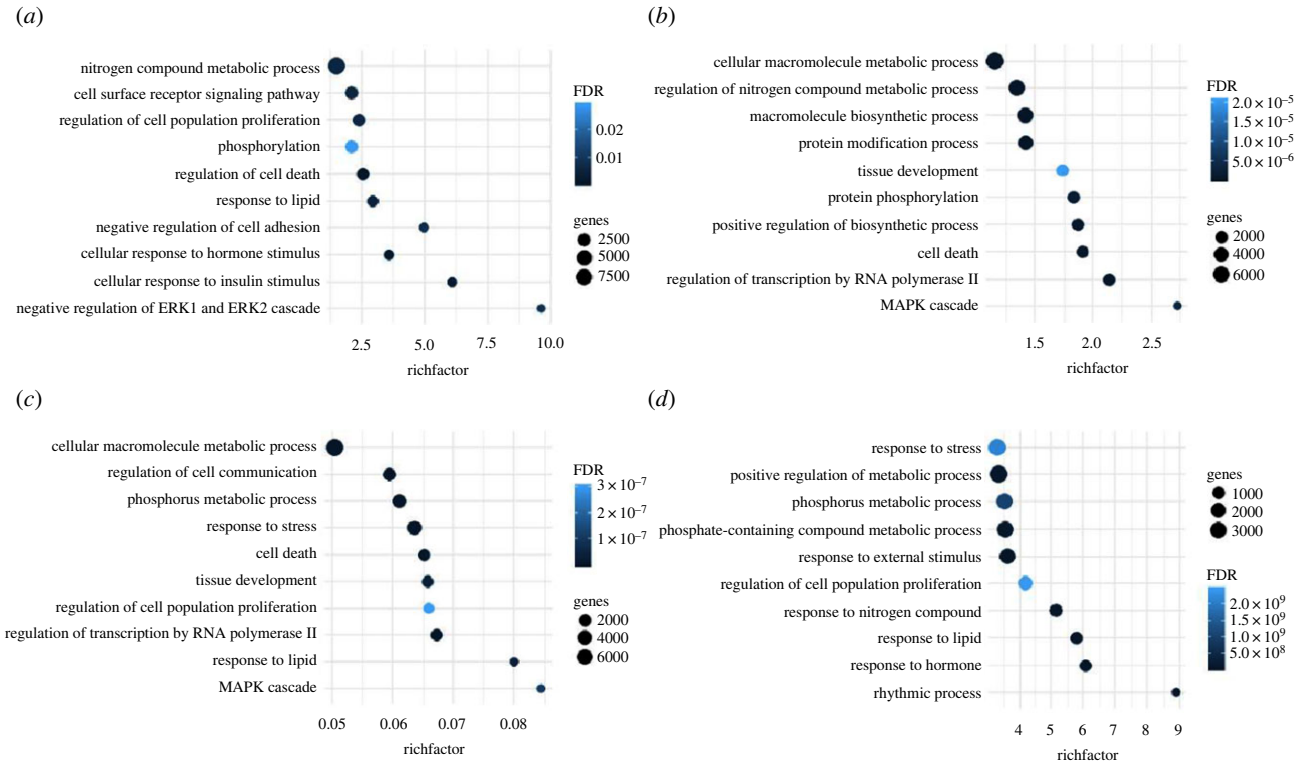

Figure 2. Selection of biological processes (GO) with high richfactor in gene set enrichment analysis for DEGs with FDR < 0.01. Selection of visualized terms was based on richfactors and occurrence in literature (full results can be found in electronic supplementary material, table S3). The size of the dots indicates the number of genes found in the GO respective term, and the richfactor reflects the proportion of genes in a given pathway. The colour indicates the FDR of the term. (*a*) SE versus TL, (*b*) TL versus AE, (*c*) SE versus AE and (*d*) SE versus TL and AE.

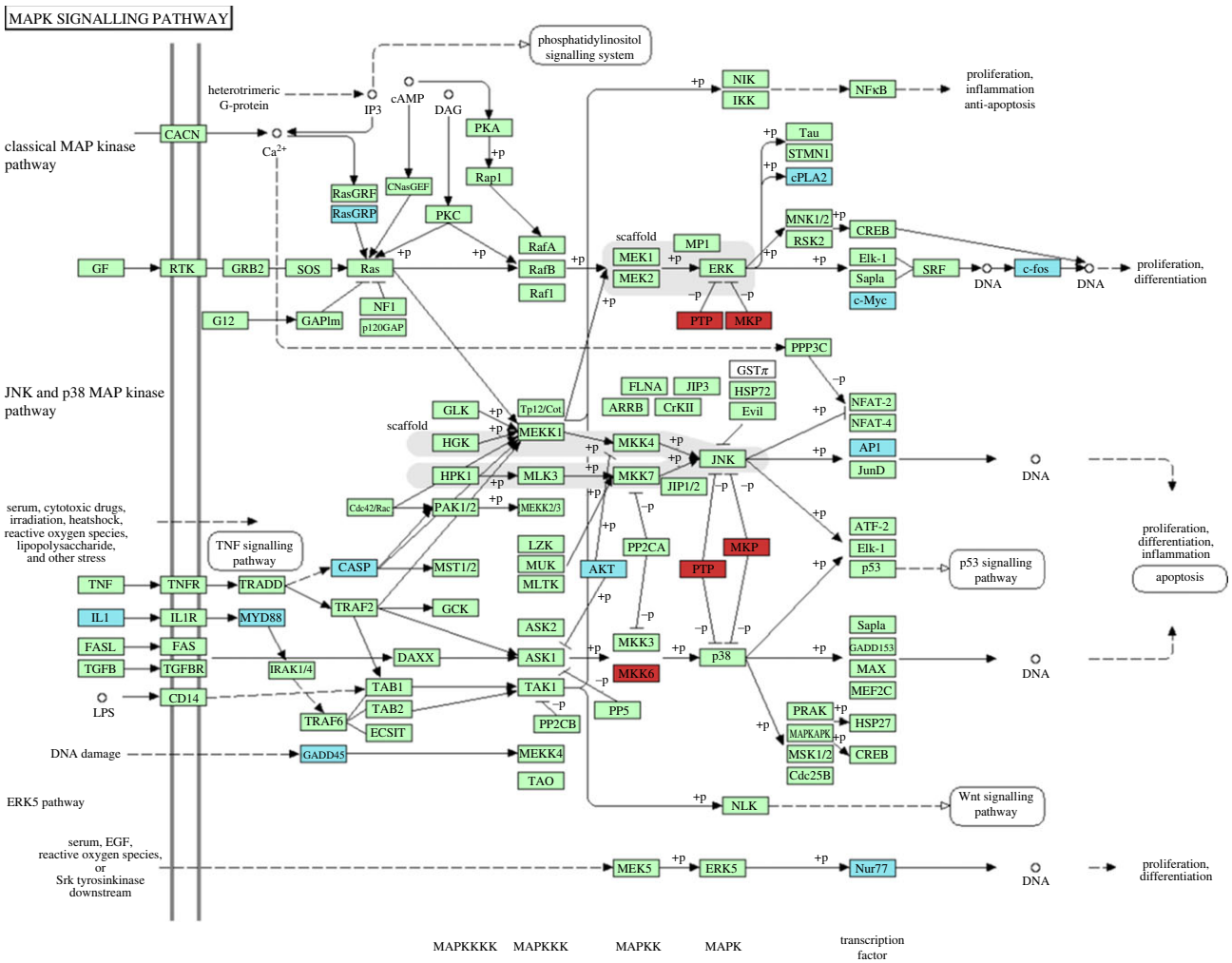

Figure 3. MAPK pathway (KEGG) with DEGs in torpor (TL) compared to SE or AE. 'MAPK(K(K(K)))' and 'TF' at the bottom of the figure indicate the type of gene product that is found above. Colour code: red = upregulated in torpor, blue = downregulated in torpor, green = not differentially expressed or not detected.

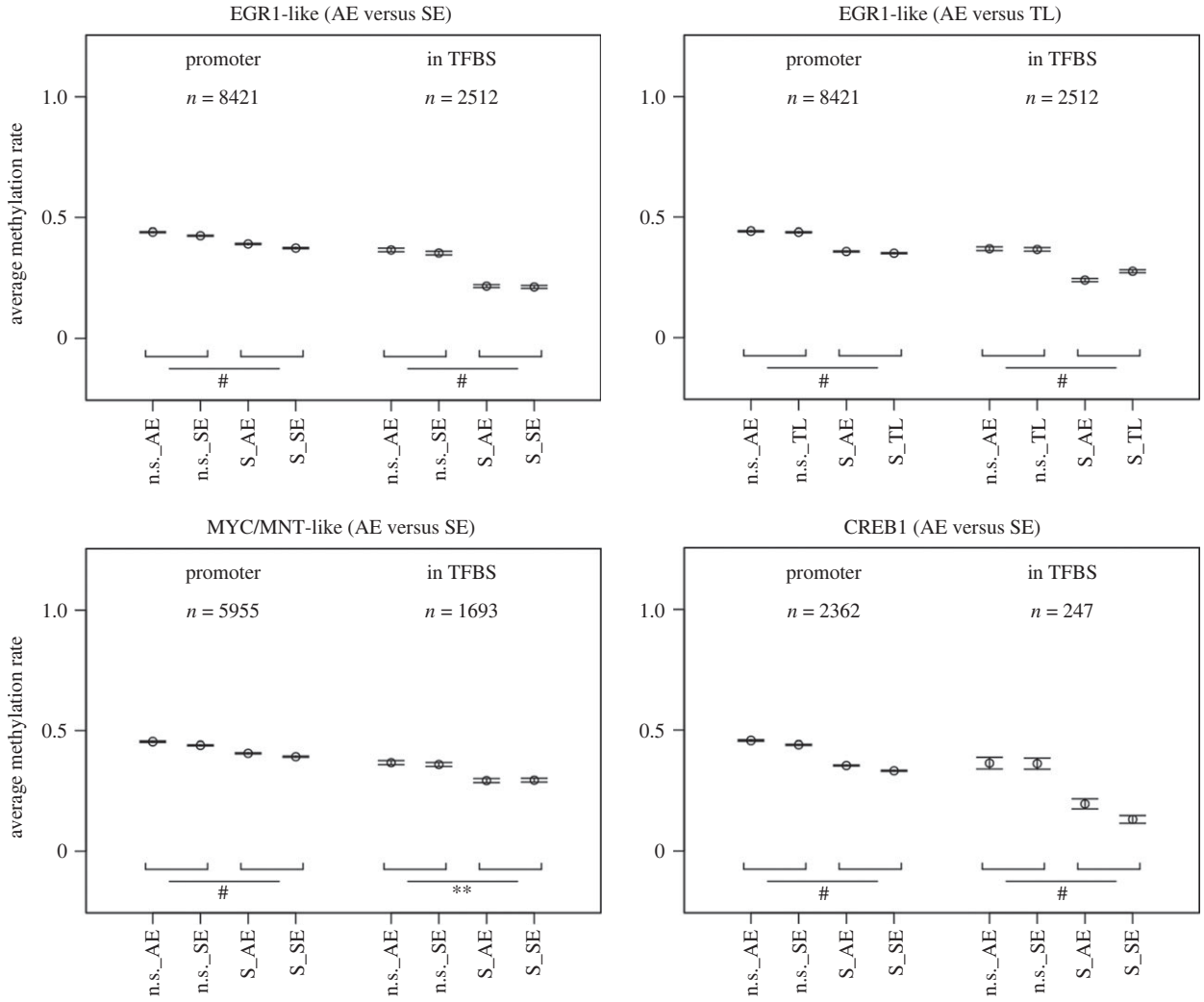

Figure 4. Methylation levels of the promoter (left) and TFBS (right) of identified TFs. (*a*) EGR1-like TF (SE versus AE). (*b*) EGR1-like TF (TL versus AE). (*c*). MYC/MNT-like TF (SE versus AE). (*d*) CREB1 TF (SE versus AE). Significance bars indicate the significance of the difference in methylation in function of hibernation state (SE, AE or TL) and differential expression state (NS or S) taken in account in the mixed models (see §4) with $^{*}p < 0.1$, $^{**}p < 0.01$, $^{***}p < 1 \times 10^{-3}$ and $^{\#}p < 1 \times 10^{-4}$; n.s. = non-significant, S = significant.

S2). The MAPK pathway relays mitogenic signals promoting cell division and proliferation. The suppression of the ERK1/2 cascade members in torpor probably relates to the arrest of the cell cycle, as denoted by the upregulation of cyclin-dependent kinase inhibitor 1 (*P21*^{CIP1}/*CDKN1A*) and of cell death-regulating genes Caspase 3 and programmed death-ligand 1 (*CD274*; electronic supplementary material, table S1). Such proposition is in line with cell cycle arrest in ground squirrel liver by reduced cyclin D and E protein levels and upregulation of cyclin-dependent kinase inhibitors (*P15*^{INK4b} and *P21*^{CIP1}) [7].

(c) Gene ontology analysis reveals repression of phosphorylation and RNA expression in torpor

GO analysis uncovered phosphorylation (terms: [protein] phosphorylation and phosphorus metabolic process; figure 2*a–d*) as a recurring pathway in all contrasts. As aforementioned, members of large phosphatase families, such as PP1 subunits, were differentially expressed in torpor. Genes downregulated in torpor, showed a clustering of *PP2A* genes, including protein tyrosine phosphatase non-receptor type 1, beta-2-adrenergic receptor and Smg5 nonsense-mediated mRNA decay factor (electronic supplementary material, table S1). PP1 and PP2a constitute large phosphatase families that are responsible for most of the serine/threonine dephosphorylations, controlling an array of processes, including metabolism and cell cycle.

The expression of DEGs related to 'regulation of transcription by RNA polymerase II' showed a mildly reduced expression in torpor and strong increase in arousal. RNA polymerase II is a multi-protein complex and one of the three eukaryotic nuclear RNA polymerases that transcribe DNA into precursors of messenger RNA (mRNA), most small nuclear RNA and microRNA. GO:cellular component (CC) reflects activation of the gene transcription machinery by terms including 'nucleus', 'nuclear part' and 'nuclear lumen', consistent with the previously reported reduction of RNA transcription in torpor [21]. Collectively, our data indicated that RNA transcription in hamster is reduced during torpor, followed by an overexpression of RNA transcription in AE.

(d) Gene ontology terms specific for one hibernation stage

DEGs for comparison of AE versus SE were enriched for GO terms 'regulation of cell population proliferation' and 'cell death'. Cell death includes apoptosis, necrosis and autophagy. Of note, a large fraction of DEGs within these terms

is related to (extrinsic) apoptotic pathways, suggesting this is a key mechanism activating the apoptosis pathway in arousing hamster liver. In hibernating hamster, an increase in cell damage marker abundance was found in torpid lung [22], which was rapidly reversed upon arousal. The latter is also suggested by observations in seasonal hibernators, such as the ground squirrel, who arrest cell proliferation in torpor without increased levels of cell death [7]. Lastly, in the AE versus SE comparison, 'metabolic responses' and 'nitrogen metabolic compound'-related terms are among the most enriched GO terms. These showed increased activity during early arousal, possibly making up for protein damage or loss during the torpor stage. Nitrogen metabolic processes generally reflect protein degradation. In ground squirrels, it has been shown that ubiquitination of proteins continues in torpor, whereas proteolysis is inhibited, which may result in increased protein degradation in arousal [23]. Likewise, in Syrian hamster, autophagy is enhanced during early arousal in heart tissue [24], presumably to clear damaged proteins.

(e) Differentially expressed genes showed minimal promoter DNA methylation differences

To interrogate whether differential DNA methylation constitutes an underlying factor driving expression changes throughout hibernation, we performed whole-genome bisulfide sequencing (WGBS) on liver DNA of these Syrian hamsters. Differentially methylated region (DMR) analysis of the DEGs (2.5 kb promoter and within-gene regions; ±4.5% of all loci) resulted in respectively 49, 57 and 45 clusters (containing greater than or equal to 2 CpGs) retained for the contrasts SE versus TL, SE versus AE and TL versus AE (electronic supplementary material, table S3). After additional filtering on DMRs featuring an average methylation difference of greater than 20%, (i) only three DMRs were retained for SE versus TL: homeodomain interacting protein kinase 2, secreted and transmembrane protein 1A and aquaporin 3; (ii) none for SE versus AE; and (iii) four DMRs for TL versus AE: *GCK*, Smad nuclear-interacting protein 1 and *GM14137* (and one gene without gene symbol: ENSMAUG00000016923). These results demonstrate at most limited evidence for changes in DNA methylation of promotor regions as a driving force of differential gene expression.

(f) Transcription factor-binding site analysis identified candidate regulatory transcription factors in arousal animals

Next, to evaluate whether the expression of the identified DEGs is driven by key TFs, we performed TF-binding site (TFBS) analysis on the 2.5 kb promoter regions of DEGs. As TFBS are well conserved, the extensive dataset of human TFBS was used, which may also point towards the human homologue (see §4). TFBS analyses identified three motifs enriched (i.e. that showed an enrichment of TFBS in promoters of DEGs compared to non-DEGs) being early growth response 1 (EGR1)-like, MYC-associated factor X (MAX) network transcriptional repressor (MNT)-like and MYC proto-oncogene (MYC)-like TFs. Interestingly, these TFBS were found to be over-represented in promoters of genes which were upregulated in AE. Also the MAPK target CAMP responsive element-binding protein 1 (CREB1) was found among the top enriched TFBS in promoter regions of genes upregulated in arousal animals compared to euthermic animals (52% enrichment). CREB1 has been described as an important target of the p38 MAPK pathway in hibernating bats, and activated through post-translational phosphorylation [25], which may explain why differential expression of CREB1 is absent in our dataset.

Interestingly, EGR1 RNA expression was upregulated in AE compared to TL and SE animals (respectively 5.6- and 18.5-fold, FDR = 9.0×10^{-3} and 4.5×10^{-7}). The enrichment of EGR1 TFBS in the promoter regions of genes upregulated in AE compared to both TL and SE was 39% and 19%, respectively. Also for EGR3 and EGR4 (TFs with highly similar probability weight matrices (PWMs, i.e. binding patterns) as EGR1), higher enrichment of their binding sequences was found (see electronic supplementary material, table S4). Differential expression of EGR3 and EGR4 was not assessed as these genes were filtered out due to too low coverage. Second, RNA expression of both MNT and MYC (discussed together due to similar PWM) showed overexpression in AE versus SE (respectively 1.8- and 12.6-fold, FDR = 1.2×10^{-3} respectively 4.9×10^{-14}) and their TFBS enrichment was significant (respectively 41% and 25%) in promoter regions of genes overexpressed in AE compared to euthermic animals. Additionally, two related TFs were found enriched with highly similar PWMs: MYCN and MAX (see electronic supplementary material, table S5). Other enriched (and depleted) TFBS can be found in electronic supplementary material, table S4.

(g) Evidence for DNA methylation modulating transcription factor activity

Despite identification of interesting TFs, overall enrichment of their binding sites in promoters of DEGs was modest. The low enrichment of TFBSs in promoters of DEGs suggests that only a limited number of target genes of these TFs are hibernation-associated. Therefore, we set out to assess the influence of DNA methylation on gene expression, focusing on those genes with the identified motifs in their promoter regions. CREB1, EGR1 and MNT/MYC were chosen due to their binding sequence enrichment and differential expression (and possible activation by phosphorylation in the case of CREB1). As all TFBS for these genes contain at least one CpG dinucleotide, DNA methylation may modulate the impact of the TF, i.e. that a relevant fraction of putative TF target genes is not differentially expressed due to DNA methylation blocking the TF-induced expression. Methylation levels of the target genes for our selection were investigated by calculating average promoter methylation as well as TFBS methylation for both DE and non-DE putative target genes. Methylation differences of DE and non-DE target genes were determined for the comparisons between hibernation stages which revealed TFBS enrichment among DE genes: i.e. (i) SE versus AE for EGR1-like, (ii) TL versus AE for EGR1-like, (iii) SE versus AE for MYC/MNT-like and (iv) SE versus AE for CREB1. For each comparison, mixed models showed significantly higher AE promoter methylation for candidate target genes that were not differentially expressed (all $p < 1.3 \times 10^{-06}$), an effect that was even more outspoken when considering methylation of the TFBS directly (figure 4; all $p < 3.6 \times 10^{-05}$, except for MYC/MNT, $p = 0.07$). Additional visualization with violin plots (see electronic supplementary material, figure S2 for average

promoter methylation and electronic supplementary material, figure S3 for average methylation in TFBS) indicates that this increase in average methylation can be particularly attributed to complete methylation of a subset of non-responding TF target genes. These results provide additional evidence for the relevance of these TFs, as the limited enrichment of their targets may be explained by the inhibitive effect of DNA methylation for non-responding TF target genes.

3. Discussion

This study is the first to investigate gene expression and its regulation in a facultative hibernator, the Syrian hamster, in an unbiased approach focusing on liver because of its critical role in metabolism, endocrinology and detoxification. Differential RNA expression analysis between all different groups revealed 619 annotated hamster genes, reflecting the dynamic nature of the transcriptome in hibernating liver. The pathways regulated throughout the hibernation cycles (SE versus TL versus AE) involve metabolic processes and transcription. These pathways correspond with those previously documented by RNA-seq and targeted metabolomics in the liver of seasonal hibernators [6,21,26–32] and activity assays in facultative hibernators [33]. Interestingly, our data showed three additional, prominently regulated pathways in hamster liver: the MAPK/ERK pathway, PP1 pathway and processes involved in cell 'life-and-death' (cell cycle, division, proliferation and death). TFBS analysis identified four candidate TFs involved in regulation of gene expression of which three were differentially expressed. Moreover, methylation of promotor regions does not associate with overall differential gene expression, yet may inhibit the responsiveness of specific genes to the identified TFs.

All hibernators (partially) switch from carbohydrate to lipids as their primary fuel source during their hibernation period. In keeping, our data indeed show upregulation of genes involved in gluconeogenesis and glycogenolysis during torpor. Glucose metabolism is regulated through limiting storage of glucose into glycogen by downregulation of three regulatory subunits of PP1 [14], which corresponds to our data in TL and AE hamsters. The limited glucose conversion is possibly induced to maintain stable glucose levels in the hibernating hamsters. Additionally, insulin resistance during torpor leads to an impaired glucose metabolism while glycogen storage is increased [14]. Simultaneously, shifts in gene expression promote glucose retrieval from glycogen through upregulation of *GAA*, a gene encoding an essential protein for glycogenolysis, in TL versus SE animals. A decrease in hepatic glycogen and upregulation of other glycogenolysis-inducing enzymes (*PYGs*), but not upregulated hepatic *GAA* expression, has been demonstrated before in hibernating animals [9]. Collectively, the regulation of genes involved in glucose-saving and glycogen-storing processes likely serve to maintain steady blood glucose throughout all hibernation stages. Moreover, the break on glycolysis observed during torpor, as demonstrated here by the strongly reduced expression of its rate-limiting enzyme, *GCK1*, is released in early arousal. The reduction of glycolysis through the downregulation of *GCK1* has been shown in other hibernators, such as grizzly bears and Asiatic black bears [5,34].

Regulation of protein phosphorylation constitutes an important category of our identified DEGs, represented in all comparisons, including the regulation of *PP1* subunits addressed above. The downregulation of genes involved in the PP1 pathway is not unexpected, as it is known in the hibernation field that both PP1 and PP2 are regulated: decreased activity of PP1 and PP2a in torpid squirrels was reported in liver and brain, respectively [35,36], and increased PP2c activity was found in skeletal muscle, brown adipose tissue, kidney, brain and liver [35,37]. Temperature does not seem to influence PP1 enzyme activity in hibernators, suggesting that PP1 regulation is an active process rather than passively regulated by reduced temperature [35]. We here report reduced mRNA expression of PP1 members, which may decrease enzyme activity in the liver during hibernation, although studies in PP1 activity in hamster liver should be conducted to confirm this hypothesis.

Remarkably, the MAPK/ERK pathway, constituting the most prominently regulated phosphorylation cascade, shows upregulation for a large number of its inhibitors (DUSPs and sproutys (SPRYs)) in torpor and arousal compared to SE. Strikingly, this strong transcriptional inhibition of the MAPK pathway has not been identified previously in hibernators. Conversely, the limited number of studies on phosphorylation status of MAPK pathway proteins show contradicting results. Increased phosphorylation of several MAPK members in liver of the obligatory hibernator Monito del Monte (*Dromiciops gliroides*) suggests the activation of MAPK signalling during torpor [38]. Also in torpid Syrian hamster brains, ERK1 phosphorylation was increased. On the other hand, in the same torpid hamsters, inhibition of the MAPK pathway was observed, indicated by a strongly reduced ERK2 phosphorylation, questioning the overall activity of the MAPK kinase pathway in these animals [39]. In torpid ground squirrel skeletal muscle, the p38MAPK2, MAPAPK2, displayed reduced activity [40]. Our data clearly showed an upregulation of MAPK pathway inhibitors in torpor and arousal at the RNA level. In combination with the observation of several downregulated genes in the MAPK pathway during torpor and arousal, this provides a strong indication that the MAPK pathway is downregulated in general, which is in contrast with the torpid hamster brain, as reported previously [39].

Among the plethora of pathways influenced by MAPK and PP1, regulation of cell cycle arrest, cell replication and cell death constitute prominent pathways regulated at the RNA level in hibernating Syrian hamster liver. Our data provide strong evidence for the marked regulation of expression of genes involved in cell 'life-and-death', including cell division and proliferation, cell cycle arrest and apoptosis. Most studies on cell division in hibernation have been carried out on gut, showing a cessation of mitotic activity in torpor, with a progression in G_1 phase but a block in G_2 or S phase [41]. Also in liver of ground squirrels, cell cycle progression was suppressed during torpor as indicated by western blot and PCR for cell cycle markers [7]. Mitotic activity and cell proliferation resume during arousals [42]. Similar to ground squirrels, our data showed an upregulation of many TFs and effectors involved in cell cycle regulation in the transition from TL to AE. Upregulated genes included the clock gene Per1, which regulates cell growth and DNA damage control [43], and a number of genes encoding FOS and jun proto-oncogene proteins, which are downstream components of the MAPK pathway and part of the AP-1 TF process. MAPKs activate the AP-1 TF complex which regulates cell growth and differentiation as a response to stress factors [44]. The likely inhibition

of the MAPK pathway throughout torpor and partially in arousal may thus serve as a regulatory mechanism to suppress the energy costly process of cell proliferation [45].

Our TFBS analysis identified six TFs potentially involved in upregulating gene expression in arousal. For three of these, we could demonstrate a differential upregulation at the RNA level in arousal (EGR1, MNT and MYC), whereas MYCN, MAX and CREB1 were not differently expressed. TFs are known to be regulated also at the post-translational level and can form complexes: MYCN belongs to the same TF family as MYC and MAX is known to form heterodimers with MYC [46,47]. Interestingly, some of the identified TFs were previously found upregulated in the liver of arousing ground squirrel (MYC) and activated in muscle of the torpid brown bat and in multiple organs (including liver) of the torpid ground squirrel (CREB1) [6,25,48], further supporting a role for these TFs in hibernation. Notably, the MAPK pathway regulates the activities of several TFs through phosphorylation, including the activation of MYC and CREB1 [49,50], revealing a possible additional role of the prominent MAPK regulation in hibernating animals. It is important to mention that the gene expression of MAPK members does not necessarily represent the activity of the MAPK enzymes. Altogether, our results suggest that the MAPK pathway plays a role during the arousal phase through the upregulation of TFs and gene expression of members of the MAPK pathway.

To further explore regulatory mechanisms in hibernation, DNA methylation was measured in the liver from the hamsters. Evidence for cyclic DNA methylation [51] and regulation by DNA methylation of cyclic processes, e.g. circadian rhythm [52], further support a possible role for DNA methylation in regulation of dynamical processes. Charting of the DNA methylation on a genome-wide level did however not show pronounced differences in liver between the hibernation groups, similar to ground squirrel. Contrastingly, DNA methylation in skeletal muscle of ground squirrel did show lower levels of DNA methylation in TL and arousal [53]. This suggests a tissue-specific role for DNA methylation in hibernation. In this respect, another study showed contrasting results in liver, kidney and heart of the chipmunk (*Tamias asiaticus*) by presenting hypomethylation of the USF-binding site in the hibernating livers, which is responsible for upregulation of the hibernation-associated *HP-27 gene*, but showed hypermethylation in kidney and heart [54]. Tissue-specific DNA methylation could explain the differences in gene expression among tissues during hibernation [5,55]. Despite the similar levels of methylation genome-wide, further investigation of the methylation status showed that promoters of non-responding (not differentially expressed) target genes have significantly higher methylation. Even more strikingly, when focusing on the transcription binding site, this effect is further enhanced. We note that most candidate-regulating TFs are overexpressed during arousal, possibly facilitating the switch from hibernating tissue to metabolically active tissue. Finetuning of this switch is probably subject to modulation by DNA methylation. Further characterization of these epigenetic differences could lead to gene-targeting therapies (e.g. epigenetic editing) enabling more effective organ transplantation.

We are aware of the current limitations of this study. Although power appears to be sufficiently high to detect significant and robust results for differential analysis, addition of more samples in our analyses might increase power to detect additional results both for differential expression and differential methylation analysis. Furthermore, current findings are limited by the experimental design presented here (i.e. identification of reported molecular mechanisms might be specific for liver tissue and facultative torpor). Further research can confirm our results and evaluate generalizability for other tissues and hibernators.

In summary, our study identifies that the facultatively hibernating Syrian hamster shares the regulation of key processes with seasonal hibernators, principally comprising metabolic changes, representing a preference for fatty acid oxidation and glucose-deriving processes. Our data implicate substantial expression changes in genes effectuating protein phosphorylation and discloses a profound transcriptional inhibition of the MAPK and PP1 pathways during torpor, of which the latter pathway has not been associated with hibernation before. The inhibition of these pathways seems strongly linked to cell cycle arrest and cessation of RNA transcription during torpor, both of which are restarted in early arousal accompanied with an overshoot in the expression of TFs. During early arousal, it is suggested that restoring the expression of MAPK members leads to activation of TFs, such as MYC and CREB1, which is facilitated by hypomethylation. Furthermore, torpid animals tolerate hepatic ischaemia following profound reductions of blood flow, while maintaining mitochondrial respiration, bile production, and sinusoidal lining cell viability, as well as lowering vascular resistance and Kupffer cell phagocytosis [56,57]. Our data provide further indications that administration of MAPK inhibitors might protect from cell damage by arresting cell cycle during ischaemia [58] and that MAPK-regulated TFs may be interesting targets to avert damage by regulating cell cycle progression during organ reperfusion. Understanding molecular hibernation mechanisms may advance therapeutic approaches in medical conditions which are strongly correlated with reduced metabolism such as ischaemia-reperfusion and transplantation.

4. Material and methods

(a) Animals

Experiments were performed on male and female Syrian hamsters (*M. auratus*) as previously described by Wiersma *et al.* [24], approved by the Animal Ethical Committee of the University Medical Center Groningen (DEC 6913B) and carried out in accordance with European and Dutch legislation. Furthermore, the study is reported in accordance with ARRIVE guidelines (https://arriveguidelines.org), and all methods were performed in accordance with relevant guidelines and regulations. The following groups were included: SE, TL (torpor > 48 h) and AE (rewarming for 90 min). Euthermic animals and hibernating animals were respectively housed at an ambient temperature of 21 and 5°C. All hibernating animals were kept in darkness until euthanization. Arousal was induced at greater than 3 days of torpor by gentle handling. The animals' activity pattern accurately identified torpor bouts of hamsters [59], as evidenced by mouth temperature (Tm) at euthanization, being 9.0 ± 0.9°C and 35.0 ± 2.1°C for TL and AE, respectively, whereas SE animals had a Tm of 35.7 ± 0.5°C. Individual sample characteristics can be found in the electronic supplementary material, table S7). Liver was flushed with physiological salt solution, removed and snap-frozen in liquid nitrogen and stored at −80°C.

(b) RNA-sequencing library preparation

Total RNA was extracted from liver tissue samples of three animals per hibernation phase using Nucleospin (Machery Nagel,

Düren, Germany). Concentrations were measured using Nanodrop and processed for RNA-seq by NXTGNT (www.nxtgnt.com). RNA quality was checked using a Bioanalyzer RNA 6000 nano chip assay and Ribogreen assay (Invitrogen, Carlsbad, CA, USA). Four hundred thirty-seven nanograms of RNA per sample was used for further analysis. cDNA libraries were prepared for sequencing using Truseq stranded mRNA library prep (Illumina, San Diego, CA, USA) according to protocol. Sequencing was performed on a NextSeq500 High output flow cell, generating single-end 75 bp reads.

(c) Transcriptome sequencing and analysis

Transcriptome sequencing produced 52.6 million reads per library (range: 40.2–62.3 M; electronic supplementary material, table S6). The reads were aligned using STAR aligner version 2.7.0f using the Ensembl reference genome MesAur1 and Ensembl 96 gene annotation. Two-pass alignment mode and gene expression quantification options were used. Out of 17 091 genes with non-zero expression, data from 11 078 genes with average expression levels above 1 fragment per million was used for analysis. Differential expression analysis was performed using EdgeR and relied on the Benjamini–Hochberg procedure for multiple testing correction [60]. Principal component analysis using covariance matrix was performed to visualize variation between animals (electronic supplementary material, figure S1).

(d) Pathway analysis/gene ontology enrichment analysis

Functional categories of DEGs (FDR < 0.01) were identified by GO analysis, categorizing DEGs in biological process (BP), molecular function and CC gene sets and by KEGG pathway analysis performed by g:Profiler (version e100_eg47_p14_7733820, using default settings) [61]. A selection of BP GO terms (based on rich factors and existing literature) were visualized by means of bubbleplots using R (version 3.6.2).

(e) Transcription factor-binding site enrichment analysis

TFBS enrichment analysis was performed as described in Diddens *et al*. [62] for promoter regions (defined as the genomic region 2000 bp upstream to 500 bp downstream of the transcription start site) of DEGs identified in transcriptome analysis (separately for up- and downregulated genes per contrast). The outgroup comprised all genes that were sufficiently covered, but not significantly differentially expressed in any contrast of interest. PWM was downloaded together with accompanying annotation from JASPAR (JASPAR 2020 server), an open source, curated database of binding motifs for TFs [63]. Since TFs are generally well conserved and the human TFBS dataset is more complete than the murine TFBS dataset (1201 versus 529 respectively, assessed on 15 January 2021), the former was selected [64]. This has the additional advantage that any TF with enrichment in predicted binding sites for a certain contrast is also present in humans and may be an interesting target for human applications. Promoters were scanned using the PWMs via the FIMO software (version 4.11.3) [65]. FIMO was run separately for each PWM due to computational limitations and all matches with $p < 1.0 \times 10^{-4}$ (default setting) were retained for quantification. After quantification, enrichment was assessed using a χ^2-test per TF binding motif and Benjamini–Hochberg correction was applied to adjust for multiple testing. TF showing enrichment with a FDR below 0.05 were considered significant. Furthermore, we focused on TF that showed significant differential expression. Upon assessment of TFs that were not significantly differentially expressed, CREB1 was included as this TF is known to be activated by phosphorylation and may thus be missed based on differential expression analysis.

(f) Whole-genome bisulphite sequencing

Total DNA from liver tissue samples was extracted using Machery Nagel Nucleospin tissue kit and used for WGBS by NXTGNT (www.nxtgnt.com). Three animals per hibernation phase (SE, TL and AE; the same individuals as used for RNA sequencing) were selected for sequencing. Concentration of the extracted DNA was measured using Quant-iT PicoGreen kit (Invitrogen). DNA quality was checked on a 1% agarose gel (E-gel EX Invitrogen). Five hundred nanograms DNA was used from each sample for further analysis. Fragmentation was performed using Covaris model S2 to obtain fragments with a size of approximately 400 bp, followed by bisulfide conversion with the EZ DNA methylation Gold kit (Zymo Research, Irvine, CA, USA) according to manufacturer's protocol. For library preparation, the NEBNext Ultra II DNA library prep kit (New England Biolabs, Ipswich, MA, USA) was used according to protocol, followed by sequencing on three Hiseq3000 lanes (Illumina), generating PE2 × 150 bp reads.

(g) Sequence read mapping, summary and differential methylation analysis

Reads were mapped using the bowtie2 option (version 2.3.3.1) of the Bismark software (Brabraham Bioinformatics, version 0.18.1_dev) against the Syrian hamster reference genome provided by Ensembl (MesAur1.0, release 95). FastQC (Brabraham Bioinformatics, version 0.11.2) was used to assess quality of the WGBS samples, indicating good quality (both on the raw and trimmed fastq files). Trim Galore! (Brabraham Bioinformatics, version 0.1.0) was used to trim out bad quality bases (quality score less than 20, default) from reads (reads trimmed shorter than 15 bp were discarded). Bismark and bismark_methylation_extractor (version 0.18.0) were used to quantify CpG methylation. Finally, coverage files were compiled (bismark2bedGraph, version 0.18.0) for downstream analysis.

The Bioconductor BiSeq (version 1.26.0) was used to import coverage files. Next, a gene-centred approach for WGBS data was performed, selecting all CpGs within DEGs or their promoter regions (defined as 2 kb upstream and 0.5 kb downstream of the transcription start site, based on Ensembl annotation). DMRs were identified as described by Hebestreit *et al*. [66] Initially, regions with 15 grouped CpGs ('grouped' meaning a maximum of 100 bp between two subsequent CpGs) and at least detected in two out of six samples are considered. Clusters were analysed and subsequently trimmed using default settings. Pairwise comparison between the three hibernation (SE, TL and AE) phases was performed. In order to obtain loci featuring robust methylation differences with a probable impact on expression, we only report results on DMRs displaying an average methylation difference of at least 20% and containing at least two CpGs (after trimming of the clusters).

(h) Methylation rates in transcription factor-binding site and promoters with transcription factor-binding site

Methylation percentages were calculated for all CpG dinucleotides that were covered at least one time in each sample ($n = 12\,405\,257$). For each candidate regulatory TF, CpGs in promoter regions of non-significantly DE and significantly DE target genes (i.e. genes with at least one TFBS in their promoter region) were selected. For EGR1 and MYC/MNT, closely related TFs were incorporated as well, since TFBS for these genes are nearly indistinguishable. Average methylation per promoter region or TFBS was modelled using a mixed model with the sample nested within the hibernation phase as a random effect and differential expression state (i.e. DE versus non-DE) of the gene as fixed effect. For graphical representation, the mean methylation per gene (after calculation

of gene-wise average over three samples for each group) and standard error on the mean are displayed.

Ethics. All animal experiments described in this manuscript were approved by the Animal Ethical Committee of the University Medical Center Groningen (DEC 6913B) and carried out in accordance with European and Dutch legislation.

Data accessibility. The datasets generated in this study are deposited in the GEO database under accession number GSE199817.

The data are provided in the electronic supplementary material [67].

Authors' contributions. L.C.: data curation, formal analysis, investigation, methodology, visualization, writing—original draft and writing—review and editing; M.M.O.: formal analysis, investigation, methodology, writing—original draft and writing—review and editing; V.G.: data curation, formal analysis and visualization; V.A.R.: formal analysis and investigation; J.J.B.: formal analysis and investigation; M.G.: investigation and methodology; H.R.B.: conceptualization, supervision and writing—review and editing; T.d.M.: methodology, supervision and writing—review and editing; M.G.R.: conceptualization, methodology, project administration, resources, supervision, writing—original draft and writing—review and editing; R.H.H.: conceptualization, methodology, project administration, resources, supervision, writing—original draft and writing—review and editing.

All authors gave final approval for publication and agreed to be held accountable for the work performed therein.

Conflict of interest declaration. We declare we have no competing interests.

Funding. This study was financially supported by a Talent PhD scholarship to M.M.O. by the Graduate School of Medical Sciences, University of Groningen, University Medical Center Groningen and two grants from the Cock-Hadders Foundation, grant nos. 2018-30 and 2019-52.

References

1. Ou J *et al.* 2018 iPSCs from a hibernator provide a platform for studying cold adaptation and its potential medical applications. *Cell* **173**, 851–863.e16. (doi:10.1016/j.cell.2018.03.010)
2. Pierro A, Eaton S. 2004 Intestinal ischemia reperfusion injury and multisystem organ failure. *Semin. Pediatr. Surg.* **13**, 11–17. (doi:10.1053/j.sempedsurg.2003.09.003)
3. Andrews MT. 2019 Molecular interactions underpinning the phenotype of hibernation in mammals. *J. Exp. Biol.* **222**, jeb160606. (doi:10.1242/jeb.160606)
4. Bai L *et al.* 2019 Hypoxic and cold adaptation insights from the Himalayan marmot genome. *iScience* **11**, 519–530. (doi:10.1016/j.isci.2018.11.034)
5. Jansen HT *et al.* 2019 Hibernation induces widespread transcriptional remodeling in metabolic tissues of the grizzly bear. *Commun. Biol.* **2**, 336. (doi:10.1038/s42003-019-0574-4)
6. Jin L, Yu JP, Yang ZJ, Merilä J, Liao WB. 2018 Modulation of gene expression in liver of hibernating Asiatic toads (*Bufo gargarizans*). *Int. J. Mol. Sci.* **19**, 1–20.
7. Wu CW, Storey KB. 2012 Pattern of cellular quiescence over the hibernation cycle in liver of thirteen-lined ground squirrels. *Cell Cycle* **11**, 1714–1726. (doi:10.4161/cc.19799)
8. Martin SL. 2008 Mammalian hibernation: a naturally reversible model for insulin resistance in man? *Diabetes Vasc. Dis. Res.* **5**, 76–81. (doi:10.3132/dvdr.2008.013)
9. Burlington RF, Klain GJ. 1967 Gluconeogenesis during hibernation and arousal from hibernation. *Comp. Biochem. Physiol.* **22**, 701–708. (doi:10.1016/0010-406X(67)90763-3)
10. Rowley JW *et al.* 2011 Genome-wide RNA-seq analysis of human and mouse platelet transcriptomes. *Blood* **118**, e101–e111. (doi:10.1182/blood-2011-03-339705)
11. Cooper S *et al.* 2021 Platelet proteome dynamics in hibernating 13-lined ground squirrels. *Physiol. Genomics* **53**, 473–485. (doi:10.1152/physiolgenomics.00078.2021)
12. de Vrij EL, Bouma HR, Goris M, Weerman U, De Groot AP, Kuipers J, Giepmans BNG, Henning RH. 2021 Reversible thrombocytopenia during hibernation originates from storage and release of platelets in liver sinusoids. *J. Comp. Physiol. B Biochem. Syst. Environ. Physiol.* **191**, 603–615. (doi:10.1007/s00360-021-01351-3)
13. Sadlon TJ, Dell'Oso T, Surinya KH, May BK. 1999 Regulation of erythroid 5-aminolevulinate synthase expression during erythropoiesis. *Int. J. Biochem. Cell Biol.* **31**, 1153–1167. (doi:10.1016/S1357-2725(99)00073-4)
14. Han HS, Kang G, Kim JS, Choi BH, Koo SH. 2016 Regulation of glucose metabolism from a liver-centric perspective. *Exp. Mol. Med.* **48**, e218-10. (doi:10.1038/emm.2015.122)
15. Reznik G, Reznikschuller H, Emminger A, Mohr U. 1975 Comparative studies of blood from hibernating and nonhibernating European hamsters (*Cricetus cricetus* L). *Lab. Anim. Sci.* **25**, 210–215.
16. Maniero GD. 2002 Classical pathway serum complement activity throughout various stages of the annual cycle of a mammalian hibernator, the golden-mantled ground squirrel, *Spermophilus lateralis*. *Dev. Comp. Immunol.* **26**, 563–574. (doi:10.1016/S0145-305X(02)00006-X)
17. Reitsema VA, Oosterhof MM, Henning RH, Bouma HR. 2021 Phase specific suppression of neutrophil function in hibernating Syrian hamster. *Dev. Comp. Immunol.* **119**, 104024. (doi:10.1016/j.dci.2021.104024)
18. Yang Z, Zhong Z, Li M, Xiong Y, Wang Y, Peng G, Ye Q. 2016 Hypothermic machine perfusion increases A20 expression which protects renal cells against ischemia/reperfusion injury by suppressing inflammation, apoptosis and necroptosis. *Int. J. Mol. Med.* **38**, 161–171. (doi:10.3892/ijmm.2016.2586)
19. Zhang S, Hulver MW, McMillan RP, Cline MA, Gilbert ER. 2014 The pivotal role of pyruvate dehydrogenase kinases in metabolic flexibility. *Nutr. Metab.* **11**, 1–9. (doi:10.1186/1743-7075-11-1)
20. Wei Z, Liu HT. 2002 MAPK signal pathways in the regulation of cell proliferation in mammalian cells. *Cell Res.* **12**, 9–18. (doi:10.1038/sj.cr.7290105)
21. Van Breukelen F, Martin SL. 2002 Reversible depression of transcription during hibernation. *J. Comp. Physiol. B Biochem. Syst. Environ. Physiol.* **172**, 355–361. (doi:10.1007/s00360-002-0256-1)
22. Talaei F, Hylkema MN, Bouma HR, Boerema AS, Strijkstra AM, Henning RH, Schmidt M. 2011 Reversible remodeling of lung tissue during hibernation in the Syrian hamster. *J. Exp. Biol.* **214**, 1276–1282. (doi:10.1242/jeb.052704)
23. Velickovska V, van Breukelen F. 2007 Ubiquitylation of proteins in livers of hibernating golden-mantled ground squirrels, *Spermophilus lateralis*. *Cryobiology* **55**, 230–235. (doi:10.1016/j.cryobiol.2007.08.003)
24. Wiersma M, Beuren TMA, De Vrij EL, Reitsema VA, Bruintjes JJ, Bouma HR, Brundel BJJM, Henning RH. 2018 Torpor-arousal cycles in Syrian hamster heart are associated with transient activation of the protein quality control system. *Comp. Biochem. Physiol. Part B Biochem. Mol. Biol.* **223**, 23–28. (doi:10.1016/j.cbpb.2018.06.001)
25. Eddy SF, Storey KB. 2007 p38MAPK regulation of transcription factor targets in muscle and heart of the hibernating bat, *Myotis lucifugus*. *Cell Biochem. Funct.* **25**, 759–765. (doi:10.1002/cbf.1416)
26. Carey HV, Andrews MT, Martin SL. 2003 Mammalian hibernation: cellular and molecular responses to depressed metabolism and low temperature. *Physiol. Rev.* **83**, 1153–1181. (doi:10.1152/physrev.00008.2003)
27. Childers CL, Tessier SN, Storey KB. 2019 The heart of a hibernator: EGFR and MAPK signaling in cardiac muscle during the hibernation of thirteen-lined ground squirrels, *Ictidomys tridecemlineatus*. *PeerJ* **2019**, 1–20.
28. Epperson E, Karimpour-Fard A, Hunter LE, Martin LS. 2011 Metabolic cycles in a circannual hibernator. *Physiol. Genomics* **43**, 799–807. (doi:10.1152/physiolgenomics.00028.2011)
29. Lin JQ, Huang YY, Bian MY, Wan QH, Fang SG. 2020 A unique energy-saving strategy during hibernation revealed by multi-omics analysis in the Chinese alligator. *iScience* **23**, 101202. (doi:10.1016/j.isci.2020.101202)

30. Nelson CJ, Otis JP, Martin SL, Carey HV. 2009 Analysis of the hibernation cycle using LC-MS-based metabolomics in ground squirrel liver. *Physiol. Genomics* **37**, 43–51. (doi:10.1152/physiolgenomics.90323.2008)
31. Staples JF. 2014 Metabolic suppression in mammalian hibernation: the role of mitochondria. *J. Exp. Biol.* **217**, 2032–2036. (doi:10.1242/jeb.092973)
32. Xiao Y *et al.* 2015 Differential expression of hepatic genes of the greater horseshoe bat (*Rhinolophus ferrumequinum*) between the summer active and winter torpid states. *PLoS ONE* **10**, 1–21. (doi:10.1371/journal.pone.0145702)
33. Chayama Y *et al.* 2019 Molecular basis of white adipose tissue remodeling that precedes and coincides with hibernation in the Syrian hamster, a food-storing hibernator. *Front. Physiol.* **10**, 1–16.
34. Shimozuru M, Kamine A, Tsubota T. 2012 Changes in expression of hepatic genes involved in energy metabolism during hibernation in captive, adult, female Japanese black bears (*Ursus thibetanus japonicus*). *Comp. Biochem. Physiol. B Biochem. Mol. Biol.* **163**, 254–261. (doi:10.1016/j.cbpb.2012.06.007)
35. MacDonald JA, Storey KB. 2007 The effect of hibernation on protein phosphatases from ground squirrel organs. *Arch. Biochem. Biophys.* **468**, 234–243. (doi:10.1016/j.abb.2007.10.005)
36. Su B, Wang X, Drew KL, Perry G, Smith MA, Zhu X. 2008 Physiological regulation of tau phosphorylation during hibernation. *J. Neurochem.* **105**, 2098–2108. (doi:10.1111/j.1471-4159.2008.05294.x)
37. Wu CW, Reardon AJ, Storey KB. 2013 Effects of hibernation on regulation of mammalian protein phosphatase type-2-A. *Cryobiology* **66**, 267–274. (doi:10.1016/j.cryobiol.2013.02.063)
38. Wijenayake S, Luu BE, Zhang J, Tessier SN, Quintero-Galvis JF, Gaitã¡N-Espitia JD, Nespolo RF, Storey KB. 2018 Strategies of biochemical adaptation for hibernation in a South American marsupial *Dromiciops gliroides*: 1. mitogen-activated protein kinases and the cell stress response. *Comp. Biochem. Physiol. Part B Biochem. Mol. Biol.* **224**, 12–18. (doi:10.1016/j.cbpb.2017.12.007)
39. Stieler JT, Bullmann T, Kohl F, Tøien Ø, Brückner MK, Härtig W, Barnes BM, Arendt T. 2011 The physiological link between metabolic rate depression and tau phosphorylation in mammalian hibernation. *PLoS ONE* **6**, e14530. (doi:10.1371/journal.pone.0014530)
40. Abnous K, Dieni CA, Storey KB. 2012 Suppression of MAPKAPK2 during mammalian hibernation. *Cryobiology* **65**, 235–241. (doi:10.1016/j.cryobiol.2012.06.009)
41. Kruman II, Ilyasova EN, Rudchenko SA, Khurkhulu ZS. 1988 The intestinal epithelial cells of ground squirrel (*Citellus undulatus*) accumulate at G2 phase of the cell cycle throughout a bout of hibernation. *Comp. Biochem. Physiol. Part A Physiol.* **90**, 233–236. (doi:10.1016/0300-9629(88)91109-7)
42. Carey HV, Martin SL. 1996 Preservation of intestinal gene expression during hibernation. *Am. J. Physiol. Gastrointest. Liver Physiol.* **271**, 805–813. (doi:10.1152/ajpgi.1996.271.5.G805)
43. Gery S, Komatsu N, Baldjyan L, Yu A, Koo D, Koeffler HP. 2006 The circadian gene per1 plays an important role in cell growth and DNA damage control in human cancer cells. *Mol. Cell* **22**, 375–382. (doi:10.1016/j.molcel.2006.03.038)
44. Shaulian E, Karin M. 2001 AP-1 in cell proliferation and survival. *Oncogene* **20**, 2390–2400. (doi:10.1038/sj.onc.1204383)
45. Lynch M, Marinov GK. 2015 The bioenergetic costs of a gene. *Proc. Natl Acad. Sci. USA* **112**, 15 690–15 695. (doi:10.1073/pnas.1514974112)
46. Grinberg AV, Hu CD, Kerppola TK. 2004 Visualization of Myc/Max/Mad family dimers and the competition for dimerization in living cells. *Mol. Cell. Biol.* **24**, 4294–4308. (doi:10.1128/MCB.24.10.4294-4308.2004)
47. Mundo L *et al.* 2019 Molecular switch from MYC to MYCN expression in MYC protein negative Burkitt lymphoma cases. *Blood Cancer J.* **9**, 91. (doi:10.1038/s41408-019-0252-2)
48. MacDonald JA, Storey KB. 2005 Mitogen-activated protein kinases and selected downstream targets display organ-specific responses in the hibernating ground squirrel. *Int. J. Biochem. Cell Biol.* **37**, 679–691. (doi:10.1016/j.biocel.2004.05.023)
49. Chambard JC, Lefloch R, Pouysségur J, Lenormand P. 2007 ERK implication in cell cycle regulation. *Biochim. Biophys. Acta Mol. Cell Res.* **1773**, 1299–1310. (doi:10.1016/j.bbamcr.2006.11.010)
50. Vanhoutte P, Barnier JV, Guibert B, Pagès C, Besson MJ, Hipskind RA, Caboche J. 1999 Glutamate induces phosphorylation of Elk-1 and CREB, along with c -fos activation, via an extracellular signal-regulated kinase-dependent pathway in brain slices. *Mol. Cell. Biol.* **19**, 136–146. (doi:10.1128/MCB.19.1.136)
51. Métivier R *et al.* 2008 Cyclical DNA methylation of a transcriptionally active promoter. *Nature* **452**, 45–50. (doi:10.1038/nature06544)
52. Peng H, Zhu Y, Goldberg J, Vaccarino V, Zhao J. 2019 DNA methylation of five core circadian genes jointly contributes to glucose metabolism: a gene-set analysis in monozygotic twins. *Front. Genet.* **10**, 1–7.
53. Alvarado S, Mak T, Liu S, Storey KB, Szyf M. 2015 Dynamic changes in global and gene-specific DNA methylation during hibernation in adult thirteen-lined ground squirrels, *Ictidomys tridecemlineatus*. *J. Exp. Biol.* **218**, 1787–1795.
54. Fujii G, Nakamura Y, Tsukamoto D, Ito M, Shiba T, Takamatsu N. 2006 CpG methylation at the USF-binding site is important for the liver-specific transcription of the chipmunk HP-27 gene. *Biochem. J.* **395**, 203–209. (doi:10.1042/BJ20051802)
55. Vermillion KL, Anderson KJ, Marshall H, Andrews MT. 2015 Gene expression changes controlling distinct adaptations in the heart and skeletal muscle of a hibernating mammal. *Physiol. Genomics* **47**, 58–74. (doi:10.1152/physiolgenomics.00108.2014)
56. Lindell SL, Klahn SL, Piazza TM, Mangino MJ, Torrealba JR, Southard JH, Carey HV. 2005 Natural resistance to liver cold ischemia-reperfusion injury associated with the hibernation phenotype. *Am. J. Physiol. Gastrointest. Liver Physiol.* **288**, 473–480. (doi:10.1152/ajpgi.00223.2004)
57. Otis JP, Pike AC, Torrealba JR, Carey HV. 2017 Hibernation reduces cellular damage caused by warm hepatic ischemia–reperfusion in ground squirrels. *J. Comp. Physiol. B Biochem. Syst. Environ. Physiol.* **187**, 639–648. (doi:10.1007/s00360-017-1056-y)
58. Darling NJ, Cook SJ. 2014 The role of MAPK signalling pathways in the response to endoplasmic reticulum stress. *Biochim. Biophys. Acta Mol. Cell Res.* **1843**, 2150–2163. (doi:10.1016/j.bbamcr.2014.01.009)
59. Oklejewicz M, Daan S, Strijkstra AM. 2001 Temporal organisation of hibernation in wild-type and tau mutant Syrian hamsters. *J. Comp. Physiol. B Biochem. Syst. Environ. Physiol.* **171**, 431–439. (doi:10.1007/s003600100193)
60. Robinson MD, McCarthy DJ, Smyth GK. 2009 edgeR: a bioconductor package for differential expression analysis of digital gene expression data. *Bioinformatics* **26**, 139–140. (doi:10.1093/bioinformatics/btp616)
61. Raudvere U, Kolberg L, Kuzmin I, Arak T, Adler P, Peterson H, Vilo J. 2019 G:Profiler: a web server for functional enrichment analysis and conversions of gene lists (2019 update). *Nucleic Acids Res.* **47**, W191–W198. (doi:10.1093/nar/gkz369)
62. Diddens J *et al.* 2021 DNA methylation regulates transcription factor-specific neurodevelopmental but not sexually dimorphic gene expression dynamics in zebra finch telencephalon. *Front. Cell Dev. Biol.* **9**, 1–19. (doi:10.3389/fcell.2021.583555)
63. Mathelier A *et al.* 2016 JASPAR 2016: a major expansion and update of the open-access database of transcription factor binding. *Nucleic Acids Res.* **44**, 110–115.
64. Nitta KR *et al.* 2015 Conservation of transcription factor binding specificities across 600 million years of bilateria evolution. *Elife* **2015**, 1–20.
65. Grant CE, Bailey TL, Noble WS. 2011 FIMO: scanning for occurrences of a given motif. *Bioinformatics* **27**, 1017–1018. (doi:10.1093/bioinformatics/btr064)
66. Hebestreit K, Dugas M, Klein HU. 2013 Detection of significantly differentially methylated regions in targeted bisulfite sequencing data. *Bioinformatics* **29**, 1647–1653. (doi:10.1093/bioinformatics/btt263)
67. Coussement L *et al*. 2023 Liver transcriptomic and methylomic analyses identify transcriptional MAPK regulation in facultative hibernation of Syrian hamster. Figshare. (doi:10.6084/m9.figshare.c.6644096)